Wave Attenuation and Tunability of a Diatomic Metamaterial

David Caballero-Russi[a], Viacheslav Slesarenko[b], Mariantonieta Gutierrez Soto[c,*]
[a]Department of Civil and Environmental Engineering, The Pennsylvania State University, 208 Engineering Collaborative Research and Education (ECoRE) Building, University Park, PA 16802 U.S.A. ORCID: 0000-0002-8250-5605;
[b]Cluster of Excellence livMatS @ FIT - Freiburg Center for Interactive Materials and Bioinspired Technologies, University of Freiburg, Georges-Köhler-Allee 105, Freiburg im Breisgau, 79110, Baden-Württemberg, Germany;
[c]School of Engineering Design and Innovation, The Pennsylvania State University, 304 Engineering Design and Innovation Building, University Park, PA 16802, U.S.A. ORC ID: 0000-0003-1609-5801; *Corresponding author. Email: mvg5899@psu.edu

ABSTRACT

The exposition level of the built environment to seismic wave propagation underscores the critical need for advanced strategies to mitigate structural damage and life-threatening conditions during earthquake events. To reduce seismic wave impact, metamaterials have unveiled promising wave attenuation performance due to their design, adaptability, and effectiveness. While numerical studies have demonstrated the effectiveness of metamaterials in attenuating different frequency excitations (including earthquake excitations), experimental evidence to corroborate wave attenuation predictions and tunable mechanisms for low-frequency waves remains limited. This research presents the evaluation of wave attenuation in a mass-and-mass metamaterial under low-frequency excitations, incorporating a tunable mechanism based on the engagement of electromagnets. The mass-and-mass metamaterial consists of a one-dimensional diatomic chain, where varying engagements of electromagnets can modify the wave attenuation effect for different tunability purposes. The dispersive behavior and frequency bandgap of the metamaterial are derived for theoretical wave attenuation. In an analytical study, the predicted wave attenuation is examined through the time-history responses and frequency response functions of analytical metamaterial models according to different engagements of electromagnets. Then, an experimental study testing a small-scale metamaterial specimen is conducted to corroborate the wave attenuation effect and its tunability in the analytical results. The results demonstrate that intentional structural modifications via the engagement of electromagnets enable adaptive solutions over wave propagation characteristics. This investigation also contributes to the development of reconfigurable metamaterials for vibration mitigation in different wave propagation problems. Consequently, new pathways for tunable and efficient wave attenuation can be envisioned in large-scale applications, including earthquake engineering.

Keywords: Wave attenuation, mass-and-mass metamaterial, diatomic chain, frequency bandgap, frequency response function, tunability, engagement of electromagnets.

1. INTRODUCTION

Earthquakes represent one of the most unpredictable and catastrophic events in communities, although they are one of the most investigated natural phenomena in structural engineering historically. The impact of seismic wave propagation on civil infrastructure has been reduced by vibration mitigation methods mainly oriented toward vibration control systems. Semi-active damping devices[1], passive isolation systems and semi-active control[2], and floor isolation systems[3], are among the most relevant research contributions to vibration mitigation methods for earthquake events. Recently, additive manufacturing of metamaterials[4] has unlocked novel, tunable wave attenuation solutions to still sustain safety requirements in structures when extreme events induced by seismic wave propagation occur. Metamaterials, artificially designed materials to achieve distinctive mechanical and dynamic properties, have demonstrated the potential to provide wave attenuation effects in earthquake engineering. By designing its internal architecture and Unit Cell (UC) arrangement, a frequency bandgap (FBG) is developed to filter wave propagation and introduce a wave attenuation effect for particular frequency ranges[5–7]. By taking advantage of this capability, multiple studies have exploited the potential of metamaterials

Multifunctional Materials and Structures, edited by Mariantonieta Gutierrez Soto, Russell W. Mailen, Fulvio Pinto, Proc. of SPIE Vol. 13433, 134330K
© 2025 SPIE · 0277-786X · doi: 10.1117/12.3054795

approaching multiple FBG designs in 3D periodic structures[8], the tunability of the FBG in metamaterials for high frequencies in elastic wave propagation[9], and noise isolation solutions for crack detection[10], to new a few. In earthquake engineering, numerical investigations on metamaterials using seismic wave shields of resonators[11], periodic inclusion arrays as barriers[12], homogenized resonator-soil layers[13], mass-in-mass lattice systems[14], and inertial amplified resonators[15] for wave attenuation performance of seismic waves have demonstrated effectiveness and potential applications.

Nevertheless, investigations on wave attenuation and tunability in metamaterial applications in engineering problems, including earthquake engineering, remain limited to high-frequency excitations, numerical studies, or fixed vibration mitigation targets. Most of these investigations present frameworks based on numerical frequency response functions (FRFs) to examine wave attenuation when structural modifications are inserted in metamaterials at high-frequency excitations[16,17]. Thus, the lack of experimental data replicating structural modifications and tunable mechanisms and limited validation of predicted numerical or analytical results are current issues to be explored further. By conducting analytical and experimental studies with tunable mechanisms, the understanding of wave attenuation and tunability in metamaterials for low-frequency excitations can be explored in more detail.

This investigation evaluates the wave attenuation of a mass-and-mass metamaterial for different low-frequency excitations and demonstrates how the engagement of electromagnets affects the wave attenuation for tunability purposes. The mass-and-mass metamaterial comprises a one-dimensional (1D) diatomic chain along with a tunable mechanism driven by the engagement of electromagnets. To predict the theoretical wave attenuation, the FBG of the metamaterial is obtained through its dispersive behavior. The time-history responses and analytical FRFs of the metamaterial model are also simulated to study the wave attenuation effect when different engagements of electromagnets are introduced. Subsequently, a metamaterial specimen is experimentally tested to determine experimental FRFs based on a small-scale laboratory setup and to corroborate the analytical predictions. By this tunability, structural modifications of the dynamic system are intentionally inserted to create modified metamaterial models and specimens, and then originate alterations in the wave attenuation effect easily (e.g., amplification). The presented wave attenuation analysis and proposed engagement of electromagnets provide relevant findings to extend metamaterial potential in wave propagation problems and to contribute to adaptive, efficient design concepts for large-scale engineering applications.

2. METHODOLOGY

The mass-and-mass metamaterial involves a periodic 1D diatomic chain evaluated at low-frequency excitations. The n^{th} UC model of the diatomic chain displayed in Figure 1 consists of two different masses, $m_1 = 0.136\,kg$ and $m_2 = 0.086\,kg$, attached one to another through a horizontal spring element with effective stiffness $k_{ef} = 2{,}400\,N/m$. Firstly, the dispersive behavior is derived to find the FBG of a diatomic infinite chain for the mass-and-mass metamaterial proposed. To demonstrate an engineering application herein, an analytical mass-and-mass metamaterial model consisting of a 3-UC diatomic chain along with an individual mass is simulated under low-frequency excitations. When a frequency sweep and forced excitations are evaluated, the displacement response of the original and modified metamaterial models is calculated according to different engagements of electromagnets. Based on this information, analytical FRFs are computed to evaluate the wave attenuation from the external excitation to the individual mass. Finally, the experimental testing of a 3-UC mass-and-mass metamaterial specimen subjected to a frequency sweep is conducted to verify the theoretical dispersive behavior and confirm the analytical results presented.

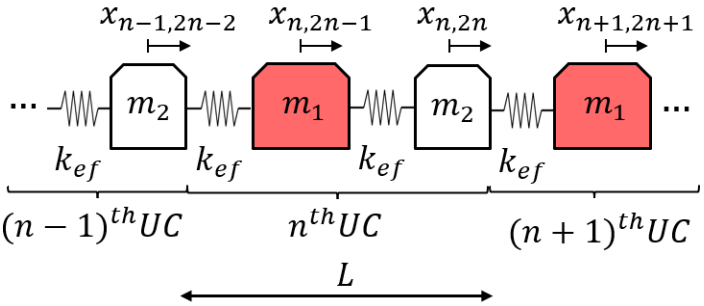


Figure 1. Dynamic subsystem of the 1D diatomic infinite chain for the mass-and-mass metamaterial

In addition to the original mass-and-mass metamaterial design, the wave attenuation analysis of two modified metamaterial models and specimens is conducted for the analytical and experimental studies. To facilitate the adoption of different engagement configurations, a tuning mechanism using the engagement of electromagnets is proposed to introduce structural modifications and derive these modified metamaterials. The engagement of electromagnets rearranges the mass and stiffness properties and impacts the periodic configuration of UCs in the mass-and-mass metamaterial. Electromagnets are inserted in mass m_1 and horizontal connectors are located at the top ends of mass m_2 and expanded up to adjacent masses m_1. A binary code representation denotes the electromagnetic force status (from external excitation to individual mass) in each UC: *0* indicates the electromagnet is disengaged (black oval), and *1* suggests the electromagnet is engaged (green oval). Figure 2 displays the interpretation of the engagement of electromagnets in the tuning mechanism proposed. For the wave attenuation analysis and tunability property of the metamaterial, the original metamaterial is considered as *0000*, and the modified metamaterials are represented as *1101* and *1111* in the analytical and experimental approaches.

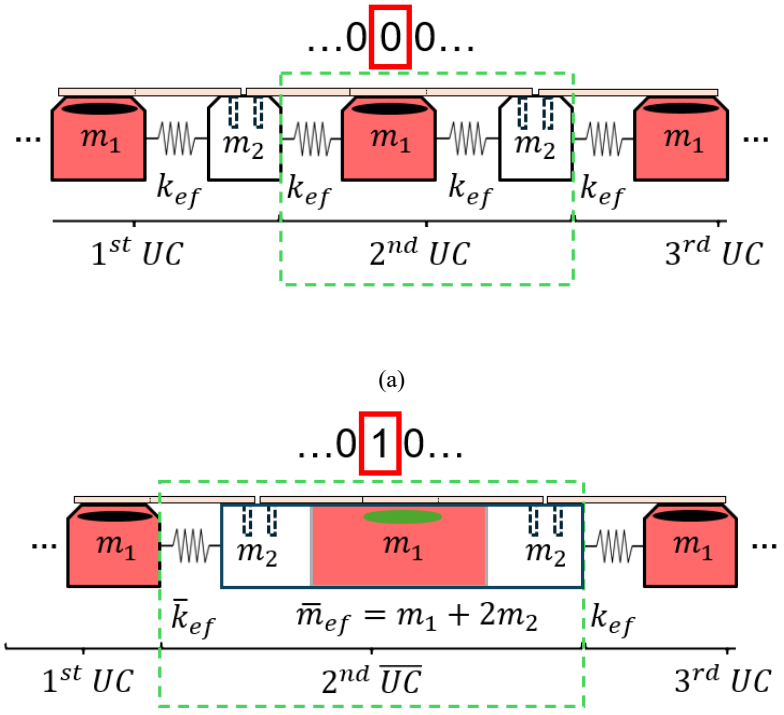


Figure 2. Interpretation of the engagement of electromagnets for the tuning mechanism proposed: (a) electromagnet disengaged (0). (b) electromagnet engaged (1).

Dispersive Behavior of Diatomic Chain

A 1D diatomic infinite chain is studied to derive the dispersive behavior of an undamped mass-spring system representing the mass-and-mass metamaterial, as shown in Figure 1 previously. Based on boundary conditions and periodicity of UCs, a dynamic subsystem of the diatomic infinite chain is analyzed to determine the mathematical expression of the dispersive behavior. To this end, a simple description of the equations of motion according to the degrees of freedom (DOF) $x_{n,2n-1}$ and $x_{n,2n}$ involved in *(n-1)*th UC, n^{th} UC, and $(n+1)^{th}$ UC is proposed through[18],

$$m_1\ddot{x}_{n,2n-1} + k_{ef}\left(-x_{n-1,2n-2} + 2x_{n,2n-1} - x_{n,2n}\right) = 0 \quad (1)$$

$$m_2\ddot{x}_{n,2n} + k_{ef}\left(-x_{n,2n-1} + 2x_{n,2n} - x_{n+1,2n+1}\right) = 0 \tag{2}$$

According to the periodic infinite chain considered, Eq. (1) and Eq. (2) are solved by Bloch's theorem presuming that waves propagate following,

$$x_{n,2n-1} = A_1 e^{i(nqL+\omega t)},\ x_{n,2n} = A_2 e^{i(nqL+\omega t)} \tag{3}$$

where i represents the imaginary unit, L corresponds to the chain constant, qL denotes the reduced wavenumber, n is the n^{th} UC, A_1 and A_2 indicate the wave amplitude of m_1 and m_2, respectively, and ω is the angular frequency. By inserting Eq. (3) into Eq. (1) and Eq. (2) and manipulating the resulting mathematical expression, a real solution for such a mathematical expression when the determinant is zero is found as[19],

$$m_1 m_2 \omega^4 - 2k_{ef}(m_1 + m_2)\omega^2 + 2k_{ef}^2(1 - \cos(qL)) = 0 \tag{4}$$

Finally, the dispersive behavior and the FBG of the diatomic infinite chain for the mass-and-mass metamaterial are obtained by solving Eq. (4) for $\omega(qL)$.

Analytical Metamaterial Study

The mass-and-mass metamaterial, consisting of a 3-UC diatomic chain along with an individual mass m_1, is simulated to predict the dynamic response and explore wave attenuation. Figure 3 indicates the analytical metamaterial model represented as an undamped 7-DOF spring-mass system.

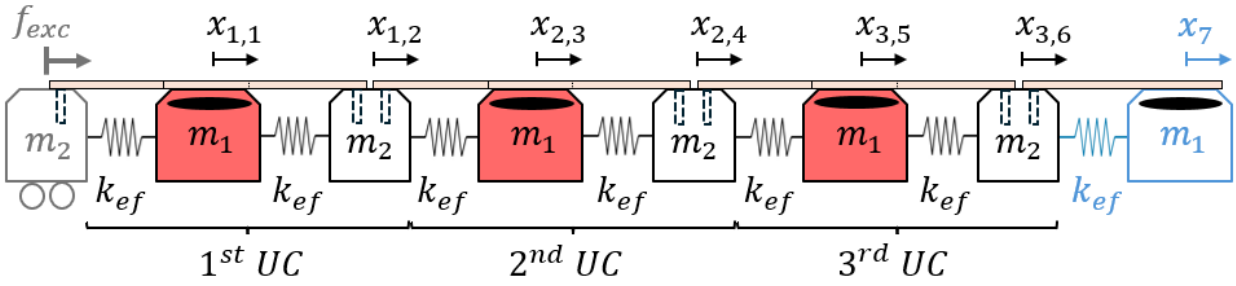


Figure 3. Analytical model of the 3-UC diatomic chain and the individual mass m_1 for the mass-and-mass metamaterial

The linear time-invariant dynamic response of the mass-and-mass metamaterial model subject to an external excitation is calculated following the classic equation of motion[20],

$$M\ddot{x}(t) + Kx(t) = F_{exc}(t) \tag{5}$$

where M and $K \in \Re^{7x7}$ indicate the mass and stiffness matrices, respectively, $x(t) \in \Re^{7x1}$ represents the vector containing the relative displacements of the system, and $F_{exc}(t) \in \Re^{7x1}$ denotes the external excitation, designated as the frequency sweep and forced excitations herein. The frequency sweep is simulated from 10 Hz to 70 Hz, while the forced excitations correspond to sine waves of 35 Hz and 15 Hz. In the frequency domain, the displacement response $u(\omega)$ of the dynamic system is written as,

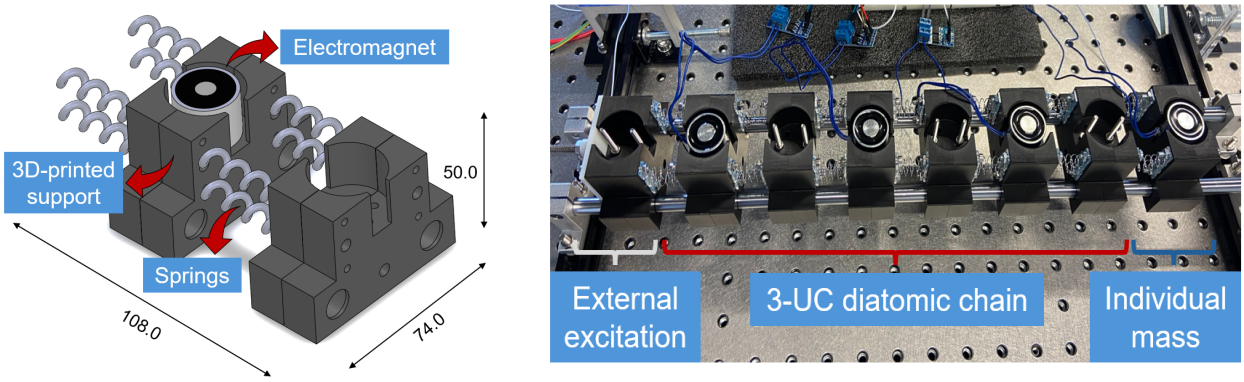
$$x(\omega) = (K - \omega^2 M)^{-1} F_{exc}(\omega) \tag{6}$$

Then, the analytical FRF is computed to explore and evaluate the wave attenuation of the mass-and-mass metamaterial model by[9],

$$Analytical\ FRF\ (dB) = 20\log_{10}\left|\frac{x_7(\omega)}{f_{exc}(\omega)}\right| \tag{7}$$

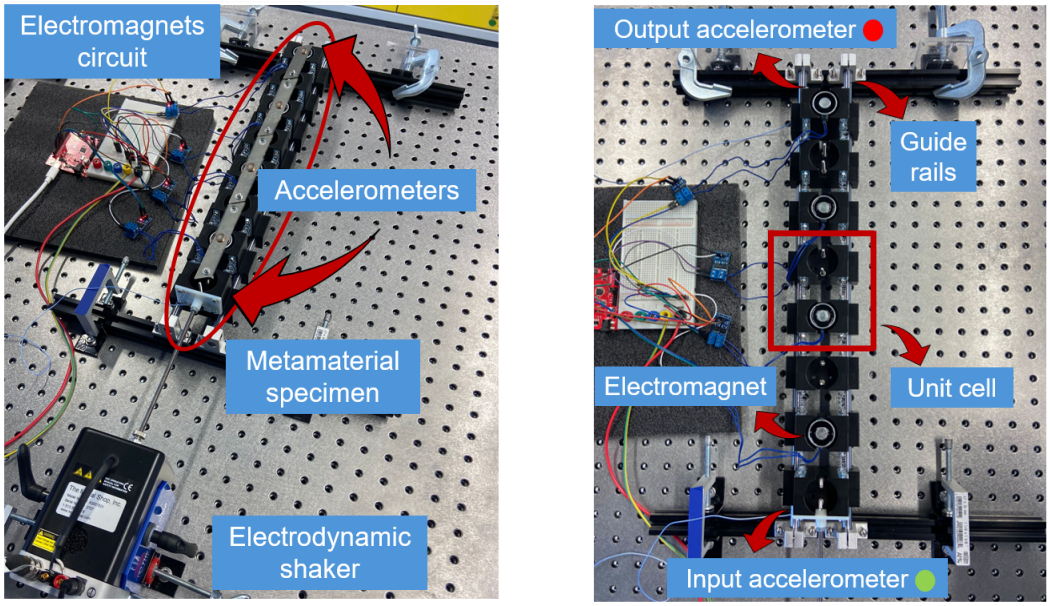
Experimental Metamaterial Study

Following the same structure described in the analytical model, a mass-and-mass metamaterial specimen is designed, additively manufactured, and tested experimentally for wave attenuation analysis. The UC design of the metamaterial specimen includes two different masses, 3D-printed supports with and without an electromagnet (m_1 and m_2, respectively), interacting periodically with one another by linear springs. Figure 4 presents the UC design and the 3-UC diatomic chain along with the individual mass m_1 assembled for the metamaterial specimen. To facilitate the arrangement and appropriate dynamic response of the metamaterial, the specimen is placed into guide rails fixed at both ends. The input excitation of this experimental test is a frequency sweep between 10 Hz and 70 Hz. The experimental setup and details of the mass-and-mass metamaterial specimen are introduced in Figure 5.



(a) (b)

Figure 4. (a) UC design in SolidWorks (units in mm). (b) 3-UC diatomic chain along with individual mass m_1



(a) (b)

Figure 5. (a) Experimental setup. (b) Details of the mass-and-mass metamaterial specimen

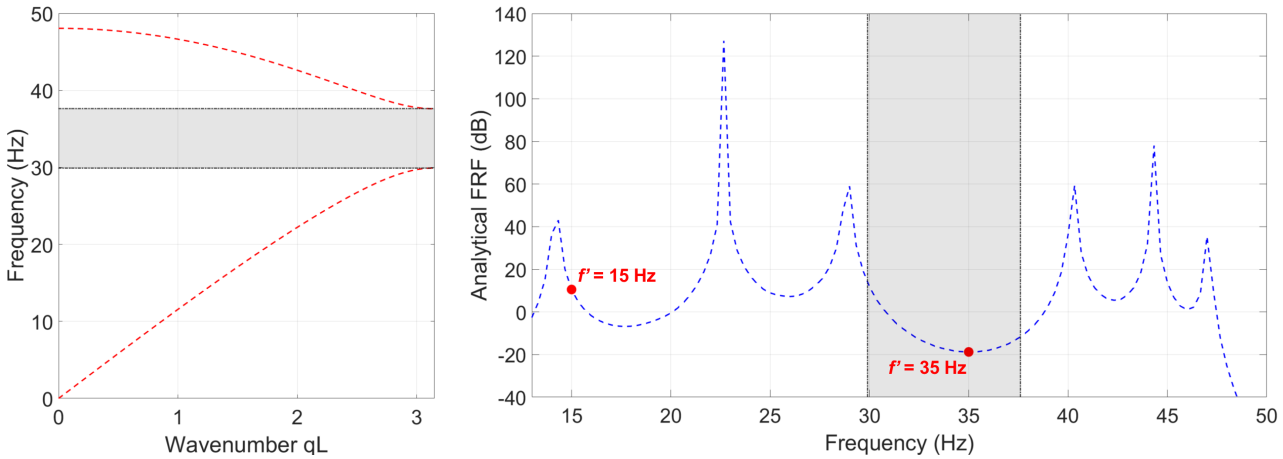
To investigate wave attenuation in experimental testing, the experimental FRF is used to explain the propagation of the incident waves across a spectrum of frequencies. The wave attenuation effect can be explored between two reference points in a dynamic system. The experimental FRF is calculated by,

$$Experimental\ FRF\ (dB) = 20\ log_{10}\left|\frac{A_{out}(\omega)}{A_{in}(\omega)}\right| \tag{8}$$

where $A_{out}(\omega)$ and $A_{in}(\omega)$ are the frequency-domain output and input signals computed by the Fast Fourier Transform, respectively. Negative FRF values express wave attenuation, and positive FRF values indicate amplification of the wave between the reference points.

3. RESULTS AND DISCUSSION

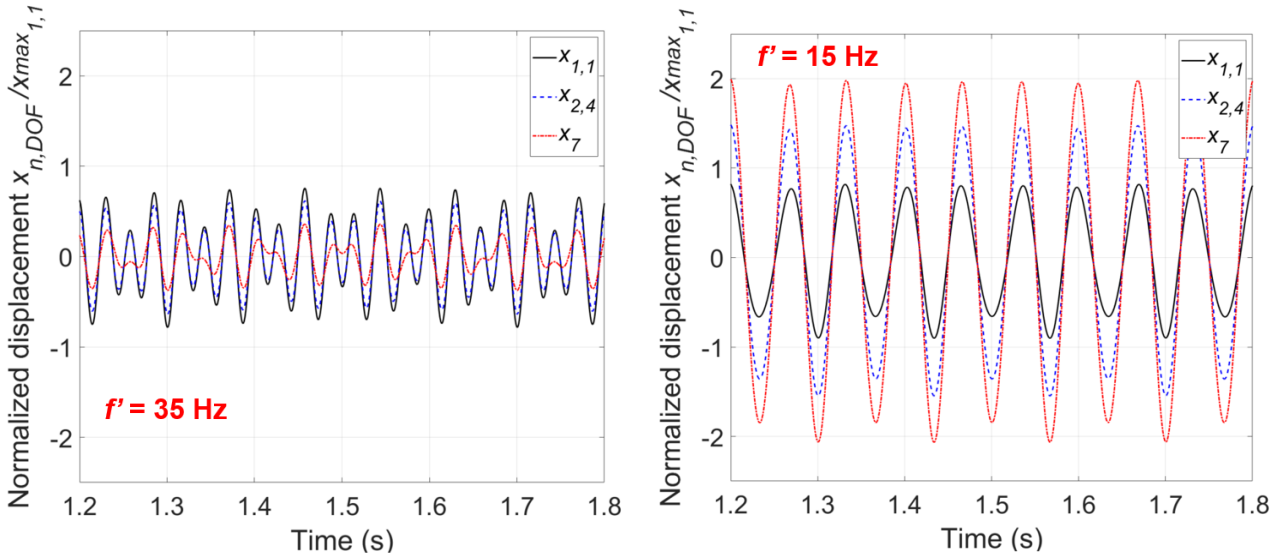
The dispersion curve for the mass-and-mass metamaterial proposed based on its diatomic infinite chain is depicted in Figure 6a. It is observed that the FBG is located between 29.9 Hz and 37.6 Hz, indicating thus the reference frequency range for the theoretical wave attenuation predicted. To corroborate analytically this attenuation property in the mass-and-mass metamaterial, the analytical FRF of the original metamaterial model subjected to a frequency sweep is calculated and presented in Figure 6b. The identified frequency limits of the strongest attenuation zone in the FRF significantly agree with the theoretical FBG limits.



(a) (b)

Figure 6. (a) Dispersion behavior of the 1D diatomic chain. (b) Analytical FRF of the original metamaterial model subjected to a frequency sweep.

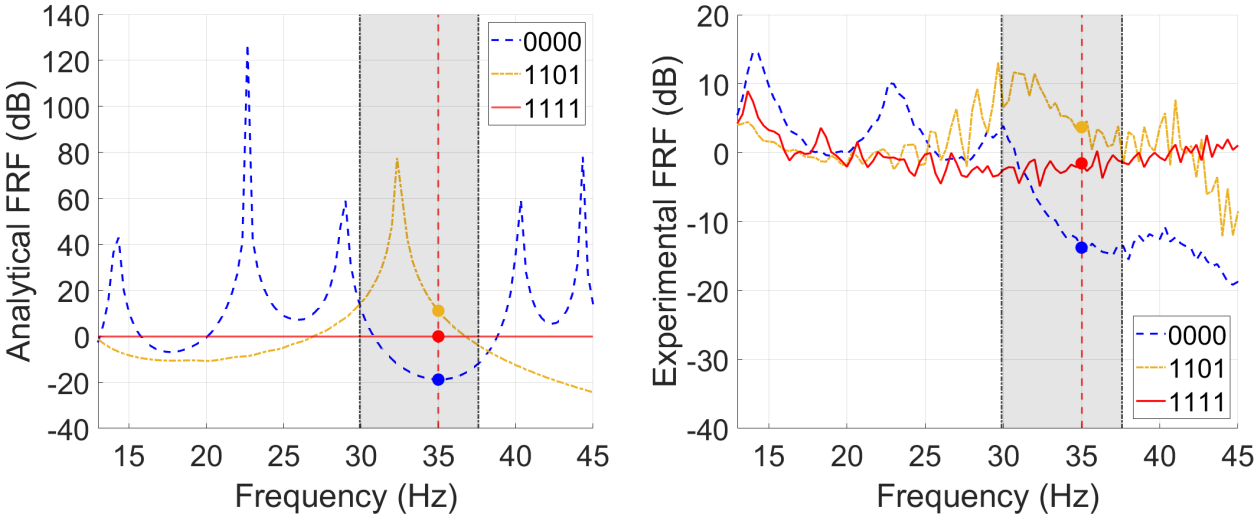
The wave attenuation effect of the original analytical model is also reflected in the time-domain displacement response of the dynamic system. For this, two forced harmonic excitations with bandgap and propagable frequencies (red dots in Figure 6b), 35 Hz and 15 Hz, respectively, are simulated to evidence the reduction and amplification of displacements at 3 DOFs. The unit-amplitude sine waves of 35 Hz and 15 Hz are simulated as external excitations. In order to normalize the dynamic responses, the displacement response of the model is divided by the maximum amplitude of $x_{1,1}$ in each forced harmonic excitation. Figure 7 introduces the normalized time-history displacement responses of the original metamaterial model for $x_{1,1}$, $x_{2,4}$ and x_7 when sine waves of 35 Hz and 15 Hz are evaluated. When the proposed metamaterial model is excited by a 35-Hz sine wave (incident wave within the FBG), the displacement response is attenuated as presented in Figure 7a. This is also noticeable by comparing it to the displacement response in Figure 7b of the same model subjected to a 15-Hz sine wave instead (incident wave outside the FBG).



(a) (b)

Figure 7. Normalized time-history displacement responses of the original analytical model for $x_{1,1}$, $x_{2,4}$, and x_7: (a) Sine wave excitation with $f' = 35$ Hz. (b) Sine wave excitation with $f' = 15$ Hz.

The tunability property of the metamaterial by the engagement of electromagnets is now evaluated. Analytical and experimental FRFs of the mass-and-mass metamaterial under 3 different engagements of electromagnets mentioned earlier are presented in Figure 8. As is observed, similar patterns are identified in the wave attenuation effect (FBG) in both analytical and experimental results as the engagement of electromagnets is performed. This is, the theoretical wave attenuation predicted can be correctly and easily evidenced at the FBG in the experimental dynamic response measured. The analytical and experimental resonance peaks of the *0000* and *1101* metamaterials demonstrate a reliable agreement. Additionally, the comparison between analytical and experimental *1111* metamaterials also confirms a proof of concept by observing the flat FRF curves. The engagement of electromagnets in such configuration poses an extreme reduction of the attenuation effect that guides the dynamic system to behave as a rigid body, facilitating propagation instead of attenuation. It should be noted that amplitude differences between analytical and experimental FRFs are mostly associated with the fact that frictional damping was not considered in the analytical model. According to these findings, it is proved that the tunability proposed in the mass-and-mass metamaterial facilitates the manipulation and modification of wave attenuation into amplification effects. This great capability shows the potential to address different wave propagation problems using the same mass-and-mass metamaterial with different engagements of electromagnets.



(a) (b)

Figure 8. Frequency response of metamaterials subjected to frequency sweep at the FBG: (a) Analytical FRFs. (b) Experimental FRFs.

4. CONCLUSIONS AND FUTURE WORK

As wave attenuation investigations of metamaterials for low-frequency excitations have been experimentally limited, the wave attenuation analysis of the mass-and-mass metamaterial studied at low-frequency excitations provides great value to the literature by effectively evaluating and comparing theoretical, analytical, and experimental approaches. The proposed tuning mechanism by the engagement of electromagnets also demonstrates the tunability potential to manipulate the wave propagation phenomenon in metamaterials. By adjusting the wave attenuation into amplification effects, the design and adaptability of metamaterials could be streamlined and exploited for multiple engineering problems simultaneously. The results of this comprehensive work serve as a pilot study to advance tunable, sustainable metamaterial solutions for wave propagation problems such as vibration mitigation for earthquake protection and wave guidance in noise control. It is noteworthy that additional modeling and testing of different engagements of electromagnets should be performed to confirm the overall attenuation effect and tunability property, and to also recognize any unknown limitations. Future work directions to be explored include analytical and experimental studies of structural health monitoring and damage detection in metamaterials[21], development of active/semi-active wave control systems driven by magnetic force[22], and investigations of wave attenuation performance considering interaction effects between metamaterials and soil media for seismic waves[23].

ACKNOWLEDGEMENTS

The authors express their sincere gratitude for the partial support provided by the Convergence Center for Living Multifunctional Material Systems (LiMC²) and the Cluster of Excellence *Living, Adaptive, and Energy-autonomous Materials Systems* (livMatS) through the Living Multifunctional Materials Collaborative Research Seed Grant Program. Additionally, the authors acknowledge partial support from the National Science Foundation (NSF) International Research Experiences for Students (IRES) Program under Grant No. 2153635.

REFERENCES

[1] Cao, L., Laflamme, S., Taylor, D. and Ricles, J., "Simulations of a Variable Friction Device for Multihazard Mitigation," Journal of Structural Engineering **142**(12) (2016).

[2] Gutierrez Soto, M. and Adeli, H., "Semi-active vibration control of smart isolated highway bridge structures using replicator dynamics," Eng Struct **186**, 536–552 (2019).
[3] Bin, P. and Harvey, P. S., "A dual-mode floor isolation system to achieve vibration isolation and absorption: Experiments and theory," J Sound Vib **525** (2022).
[4] Fan, J., Zhang, L., Wei, S., Zhang, Z., Choi, S. K., Song, B. and Shi, Y., "A review of additive manufacturing of metamaterials and developing trends," Materials Today **50**, 303–328 (2021).
[5] Gao, C., Halim, D. and Yi, X., "Elastic metamaterial with multiple resonant modes and asymmetric structure design for low-frequency vibration absorption," Acta Mech **233**(12), 5321–5333 (2022).
[6] Palermo, A., Vitali, M. and Marzani, A., "Metabarriers with multi-mass locally resonating units for broad band Rayleigh waves attenuation," Soil Dynamics and Earthquake Engineering **113**, 265–277 (2018).
[7] Zhu, D., Huang, X., Hua, H. and Zheng, H., "Vibration isolation characteristics of finite periodic tetra-chiral lattice coating filled with internal resonators," Proc Inst Mech Eng C J Mech Eng Sci **230**(16), 2840–2850 (2016).
[8] D'Alessandro, L., Belloni, E., Ardito, R., Braghin, F. and Corigliano, A., "Mechanical low-frequency filter via modes separation in 3D periodic structures," Appl Phys Lett **111**(23) (2017).
[9] Zhang, Q., Zhang, K. and Hu, G., "Tunable fluid-solid metamaterials for manipulation of elastic wave propagation in broad frequency range," Appl Phys Lett **112**(22) (2018).
[10] Kabir, M., Mostavi, A. and Ozevin, D., "Noise isolation with phononic crystals to enhance fatigue crack growth detection using acoustic emission," J Civ Struct Health Monit **8**(3), 529–542 (2018).
[11] Achaoui, Y., Ungureanu, B., Enoch, S., Brûlé, S. and Guenneau, S., "Seismic waves damping with arrays of inertial resonators," Extreme Mech Lett **8**, 30–37 (2016).
[12] Li, T., Su, Q. and Kaewunruen, S., "Seismic metamaterial barriers for ground vibration mitigation in railways considering the train-track-soil dynamic interactions," Constr Build Mater **260** (2020).
[13] Zeighami, F., Palermo, A. and Marzani, A., "LOCALLY RESONANT METAMATERIALS FOR CONTROLLING SEISMIC LOVE WAVES," Proceedings of the Eighteen World Conference on Earthquake Engineering Milan 2024, Milan (2024).
[14] Wagner, P. R., Dertimanis, V. K., Antoniadis, I. A. and Chatzi, E. N., "On the feasibility of structural metamaterials for seismic-induced vibration mitigation" (2016).
[15] Zeighami, F., Palermo, A. and Marzani, A., "Inertial amplified resonators for tunable metasurfaces," Meccanica **54**(13), 2053–2065 (2019).
[16] Kiracofe, D., Wani, U., Xu, Y. F., Kiracofe, D. and Wani, • U., "Chapter9 Damaged Metamaterials: Structural Health Monitoring and Damage Tolerance Check for updates," Conference Proceedings of the Society for Experimental Mechanics Series **2**.
[17] Zhu, Y. C., Cantero Chinchilla, S., Meng, H., Yan, W. J. and Chronopoulos, D., "Damage detection, quantification, and localization for resonant metamaterials using physics-based and data-driven methods," Struct Health Monit **22**(5), 3338–3355 (2023).
[18] Deymier, P. A., [Acoustic Metamaterials and Phononic Crystals], Springer Berlin Heidelberg, Berlin, Heidelberg (2013).
[19] Graz University of Technology., "1-d chain of atoms with two different masses," 2018, <https://lampz.tugraz.at/~hadley/ss1/phonons/1d/1d2m.php> (23 December 2024).
[20] Chopra, A. K., [Dynamics of Structures], Pearson Education, London (2012).
[21] Caballero-Russi, D., Slesarenko, V. and Gutierrez Soto, M., "STRUCTURAL HEALTH MONITORING AND ESTIMATION OF DEGREE OF DAMAGE IN LOCALLY RESONANT METAMATERIALS," Proceedings of the Eighteen World Conference on Earthquake Engineering Milan 2024, Milan (2024).
[22] Palermo, A., Wang, Y., Celli, P. and Daraio, C., "Tuning of Surface-Acoustic-Wave Dispersion via Magnetically Modulated Contact Resonances," Phys Rev Appl **11**(4) (2019).
[23] Colombi, A., Zaccherini, R., Aguzzi, G., Palermo, A. and Chatzi, E., "Mitigation of seismic waves: Metabarriers and metafoundations bench tested," J Sound Vib **485** (2020).